JOURNAL OF OPTOELECTRONICS AND ADVANCED MATERIALS Vol. 9, No. 11, November 2007, p. 3533 - 3540

Ozone profiles over the South Pole from ground-based retrievals and satellite data

A. NEMUC*, R. L. DE ZAFRA[a]
National Institute of R&D for Optoelectronics, 1 Atomistilor Street, Magurele, Ilfov, Romania
[a]Institute for Terrestrial and Planetary Atmospheres, State University of New York, Stony Brook, N.Y.,USA

We have compared vertical profiles of O_3 from a ground-based millimetre-wave spectrometer (GBMS) located at the South Pole with ozone profiles from the Microwave Limb Sounder (MLS) onboard UARS(Upper Atmosphere Research Satellite). Air parcel trajectories were used to select MLS measurements within 70°-80° S latitude and 6 days forward or backward from GBMS observations. We interpret some common features and explain discrepancies. Double-peaked vertical profiles are present for a large fraction of the year throughout the region considered. Comparisons of GBMS with zone averages of MLS data were also made, showing the clear presence of seasonal gradients in the mid to upper stratosphere when lateral transport is slow in comparison with the O_3 photochemical equilibrium lifetime.

(Received August 1, 2007; accepted November 1, 2007)

Keywords: Ozone, Measurements, Antarctica, Stratosphere

1. Introduction

In this paper we will first compare retrievals of stratospheric ozone from a ground-based remote-sensing spectrometer with those from a satellite-based remote-sensing spectrometer. Our objective is to make an intercomparison between the ground-based measurements and the satellite data which, in earlier releases, has been the subject of a number of validation studies against several other types of instrumentation (see detailed references below).

Observations by various instruments onboard the Upper Atmospheric Research Satellite (UARS) since its launch in September 1991 have added greatly to our knowledge of the chemistry and dynamics of the Antarctic vortex region. The Microwave Limb Sounder (MLS) has been especially fruitful in large scale mapping of stratospheric ozone depletion and its correlation with chlorine chemistry through concurrent observations of ClO. A number of intercomparisons have served to verify the MLS ozone data in its earlier release versions. (See Section 2 for references.) Here we make an intercomparison between Version 5 MLS ozone data and results from a ground-based instrument operating at the geographic South Pole. We first establish that results from the two instruments are generally in good agreement (within their mutual uncertainties) and then, using observations from both instruments, draw some inferences concerning behaviour of the Antarctic stratospheric vortex over its annual cycle of formation and dissipation.

A large number of studies have by now been made of various properties of the Antarctic vortex, but to date the major emphasis has been on understanding the dynamics and chemistry associated with ozone loss in the spring stratosphere, and significantly less attention has been paid to the full annual cycle of dynamics and chemistry affecting the southern vortex region. Cheng et al. [4,5] looked at two annual cycles of ozone behaviour (1993 and 1995), in part using ozone as a fall and winter tracer of vertical descent, and showed that rates of vortex subsidence inferred from O_3 mixing ratio contours were physically inconsistent between the upper and lower stratosphere, if the vortex region were assumed to be isolated from all but vertical transport.

In the course of studying the origin and diabatic descent of polar vortex air in the northern and southern hemispheres, Rosenfield and Schoeberl [18] have computed both forward and backward three-dimensional stratospheric trajectories for large ensembles of air parcels, based primarily on high resolution UKMO meteorological data. They assert that back trajectory modeling generally yields more accurate information on the origin of vortex air and its rate of diabatic descent. From back-trajectory tracing starting on October 1, 1997, for instance, from the 700 K level, they find that significant amounts of air entered the Antarctic vortex as late as May from locations between 30° and 60° S, at altitudes concentrated near 1000 K. Furthermore, it appears that about 1/3 of the air parcels within 30° of the Pole on October 1, 1997, were well to the north of 60° S as late as June 1. Unfortunately no illustrations are given for the origin of air ending at θ values higher than 700 K by the end of winter. Forward trajectory calculations starting at 1200 K on March 1 indicate considerable amounts of air leaving the vortex at all altitudes between 1200 K and ~700 K through the entire fall and winter period (March 1 to August 1) and lesser amounts leaving into the spring (to October 1). One may infer that roughly equal amounts of air must have entered the vortex stratosphere at equivalent levels throughout this period, which would constitute considerable cross-boundary transport throughout the stratosphere. In this paper we will present observational evidence that considerable transport occurs from 60° S in the mid to upper stratosphere towards the end of May and extending into June, after a period of weaker meridional transport during April and May.

2. Data coverage and analysis

A ground-based mm-wave spectrometer (GBMS) was operated at the Amundsen-Scott South Pole Station during most of a 12-month time span during the years 1993, 1995, and 1999. This spectrometer was specially developed for the observation of pressure-broadened molecular rotational lines [18], from which vertical mixing ratio profiles can be retrieved by deconvolution against atmospheric pressure profiles. The Microwave Limb Sounder (MLS) onboard the Upper Atmospheric Research Satellite (UARS) is also a millimetre-wave spectrometer, and began observations with the launching of UARS in the fall of 1991. It continued to operate, on an increasingly reduced schedule, up to the end of July 1999, when all regular observations over Antarctica were suspended.

Both the GBMS and MLS instruments retrieve vertical distributions of several different molecular species by making use of pressure-broadened rotational emission lines. Here, we consider only ozone, and will concentrate attention on comparing observations made during 1993, when the largest mutually overlapping data sets are available. Comparison will be made between retrieved GBMS mixing ratios and MLS mixing ratios at a number of different pressure levels, using results from the latest data retrieval algorithms for the MLS observations. These retrievals, known as Version 5 (V5), were made available for public use at the NASA Goddard Space Flight Center's Distribution Archive Access Center. Although no validations of the individual species data sets for V5 processing have been published yet, the V5 processing itself is described in detail by Livesey et al. [2002]. Processing details and preliminary accuracy estimates, along with much additional information, are also available on the UARS/MLS website (http://mls.jpl.nasa.gov/joe/mls_home_page/umls_V5_data_quality.txt). A separate comparison, similar to that in the present paper, has been made between GBMS HNO_3 profile retrievals and MLS Version 5 retrievals by Muscari et al. [14].

Although the retrieval of molecular mixing ratios from the GBMS and MLS observations both rely on the deconvolution of spectral line shapes from pressure broadened molecular rotational transitions, the techniques used are somewhat different in detail, dictated in part by the very different observing geometries. The MLS validation for earlier V3 ozone retrievals has been covered in detail by Froidevaux et al. [7]. Cunold et al. [6] have made profile intercomparisons between MLS V3 data, Halogen Occultation Experiment (HALOE) data, Cryogenic Limb Array Etalon Spectrometer (CLAES) data, and Improved Stratospheric and Mesospheric Sounder (ISAMS) data, all instruments on board the UARS satellite. MLS V4 retrieval quality is discussed in the World Meteorological Organization Report No. 43 [22].

GBMS ozone retrievals have been tested against local ozonesonde measurements in the lower stratosphere, and by using synthetic spectra generated from known vertical profiles in the mid- to upper stratosphere [3,4], but have not previously been directly compared with MLS retrievals.

In the current study we make use of the non-gridded Level 3AT data of Version 5. MLS V5 retrievals are given on each of the standard UARS pressure levels (defined by log(P)=1/6, i.e., 6 levels per decade of pressure; corresponding to intervals of ~3 km). MLS V5 ozone data thus have twice the pressure resolution of the V3 or V4 data, up to pressures = 0.1 hPa. MLS retrievals employ pressure as an independent variable, obtained from the United Kingdom Meteorological Office assimilation data. The GBMS retrievals are also carried out with pressure as an independent variable. This is obtained (along with temperature), from local South Pole meteorological balloon data supplemented above balloon limits by locally gridded NCEP data for the remaining stratosphere. GBMS data have been used, however, after conversion to a km height scale (using the same local meteorological data). For the present analysis, retrievals were converted back to pressure levels using the original pressure profiles. Although the different sources for pressure profiles used for MLS and GBMS ozone mixing ratio retrievals are a potential source for discrepancies in results, the probable pressure-altitude errors are small relative to the minimum height resolution of either observing system, and we moreover find no systematic errors (e.g., differences which could be reduced by a uniformly applied altitude rescaling) attributable to this source. A conversion of both data sets to a set of standard potential temperature (θ) surfaces was carried out by interpolation, so that air parcels could be followed using quasi-isentropic trajectory analysis (see Section 3 below).

At altitudes below 100 hPa (~14 km), MLS retrieved ozone values are primarily climatological and do not contain useful observational information. The GBMS retrievals, in turn, are forced to match direct (weekly) ozonesonde profiles measured at the Pole below ~90 hPa (~15 km), while the 15-20 km altitude range is influenced by the sonde measurements in decreasing proportion with increasing altitude.

The MLS originally made O_3 observations at two different frequencies – 183 and 205 GHz. The 183 GHz radiometer failed in April of 1993, and thus we have only used 205 GHz data for the comparisons made here. The MLS makes a full vertical scan (~0 to 90 km tangent height) every 65.5 s, during which the spacecraft moves about 400 km along its trajectory, perpendicular to the MLS line of sight. The more limited vertical range of interest in the present study (~15-42 km) reduces this horizontal smearing to about 120 km in the direction of the spacecraft trajectory over the time needed for this vertical coverage. Longitudinal coverage by the MLS is asymmetrical, from 34° on one side of the equator to 80° on the other during each orbit, and this pattern is reversed by a UARS "yaw manoeuvre" at approximately 36 day intervals. Near the latitude extreme of 80°, orbital trajectories converge to give a rather high spatial density of observations each 24 hours. For this reason, a good number of matches could be achieved between MLS observations at 70-80□ S and air parcels observed by the GBMS during passage over the Pole when using back or forward air-parcel trajectory tracing to select MLS observations (see below). The vertical resolution of the MLS retrievals is ~3.5 km (~110 - 120 K in the lower winter stratosphere) resulting in a mild inter-dependence

of data on adjacent V5 retrieval levels, which have about 2.5 to 3 km separation.

The GBMS makes observations of the moderately strong 277 GHz O_3 transition line, which typically yields emission spectra with a signal/noise ratio of ≥100:1 at the line centre. Retrievals of O_3 vertical distributions from the pressure-broadened line shapes are therefore only slightly degraded from the noise-free limit. The GBMS error budget and vertical resolution (~7 km for lower and mid-stratospheric O_3 observations) are discussed in detail in Cheng et al. [4].

During 1993, GBMS ozone observations were made every 2 to 3 days during most of the year, except when bad weather or instrument problems intervened. In all, high quality O_3 measurements used in the present study were made on 83 days during 1993. Integration time for the collection of spectra was about one hour, and most observations were started within 2 hours of Greenwich noon. Although alternate 36-day blocks of data are unavailable in the 70°-80° S range from the MLS, observations could be matched between the MLS and GBMS observations through trajectory tracing on about 35 days well-distributed through 1993.

3. Trajectory matching

Since the measurement locations for the two data sets are different, we have used the trajectory-matching technique [11,12] to connect air parcels passing over the Pole with locations of MLS measurements. To insure consistency in trajectories, at each potential temperature level of interest, we followed a cluster of 8 parcels, starting from within a ~100 km circle around the Pole, beginning at noon of any day when GBMS data were available. Trajectories for each cluster of parcels were run for 7 days backward and forward in time, using the Goddard Space Flight Center (GSFC) quasi-isentropic trajectory model [20]. This time span is sufficiently short to insure good reliability in trajectory tracing, and also only minor subsidence. Trajectories were followed at 12 potential temperature levels: θ = 375, 420, 465, 520, 585, 620, 655, 740, 960, 1300, 1450, and 1700 K. Occasionally, a single trajectory would depart significantly from the cluster (in less than 10 % of clusters traced) and this was rejected. An average of all good trajectories was then made on each level and these were used to select MLS data for comparison.

MLS non-gridded Version 5 Level 3 data were used limited to retrievals that passed the standard MLS quality checks. We experimented with various temporal and spatial limits within which to compare GBMS and MLS data. Periods of 2, 4, and 6 days were tried, and no statistically significance differences were seen in the MLS data sets. We also compared trajectory-matched MLS data gathered between 75°-80° S and 70°-75° S with 70°-80° S and again found no statistically significant differences. Finally, we explored various longitude limits and settled on 10° each side of the trajectory trace to insure a reasonable number of MLS data matches (see below) while still imposing fairly limited geographical bounds.

The following criteria were thus imposed to select MLS data for comparison. First, MLS must have collected data in the 70°-80° S latitude range on at least one day out of the 6 days preceding or following a GBMS measurement. We then tagged all MLS measurements which fell within a box of 5° latitude by 20° longitude (~556 by 575 km), measured from the averaged mid-day trajectory location. All observations found in this box within the appropriate altitude range were then interpolated onto the standard potential temperature level where the parcel was located and then averaged together using a $\cos2(\Delta d)$ weighting function, where Δd is the distance from the box centre (defined by the averaged trajectory). This weighting function is normalized to unity at the centre and zero at the edges of the box. Finally, those MLS observations which met the spatial selection criteria were averaged together using a $\cos2(\Delta t)$ weighting function, where Δt is the time in days between a GBMS observation and a spatially-selected MLS day of measurement. This weighting drops to zero at 7 days before or after the day of GBMS measurement. In 1993 there were 83 days when GBMS profiles were retrieved, but only on 34 to 38 days was at least one correlation found with MLS data. (The variable number of matches arises from the fact that the trajectory paths may enter the 70° to 80° latitude range at some altitudes but not at others within the time limits imposed.) The spatially and temporally averaged MLS ozone mixing ratio value obtained as described above was then compared with the GBMS profile measured at the South Pole, interpolated to each of the 12 potential temperature levels and for each day of matching data.

4. Error analysis

Cheng et al. [4] describe estimates of the limiting accuracy with which ozone profiles can be retrieved from our GBMS pressure-broadened spectral data. The total uncertainty used for simplicity in the current comparison is ±15% at each altitude. This was obtained by summing the overall uncertainties in inversion and calibration in quadrature.

Uncertainties in individual measurements in the MLS data have been taken from the Version 5 Level 3 data files. We consider these for each observation, after they have been interpolated onto standard potential temperature levels along with ozone mixing rations, and then average the errors (if more than one matching observation is present) using the same weighting as for the data. Finally, the averaged result is divided by the square root of the number of observations involved in the average. This procedure is appropriate for an average whose individual members have uncorrelated errors, which we assume to be the case for the retrieval errors arising from random noise in the MLS data.

5. Results and discussion

We present results in three different graphical forms: a selection of typical vertical mixing ratio comparisons (Figure 1); time sequences of mixing ratio comparisons at specific θ levels (Figures 2, 3, and 4). Each is useful to clarify different aspects of the comparison, and we then go on to draw attention to, and reach conclusions about, some

features involving the annual cycle of chemical and dynamical changes that affect ozone over the Antarctic region.

5.1. General results from trajectory tracing

Fig. 1a – 1b shows a selection of single profile comparisons between the two data sets. They are in chronological order). Note that since air at different levels typically travels along differing trajectories and at different speeds, the MLS profiles assembled to compare with GBMS profiles are not the same as MLS profiles determined for a specific MLS latitude-longitude grid point.

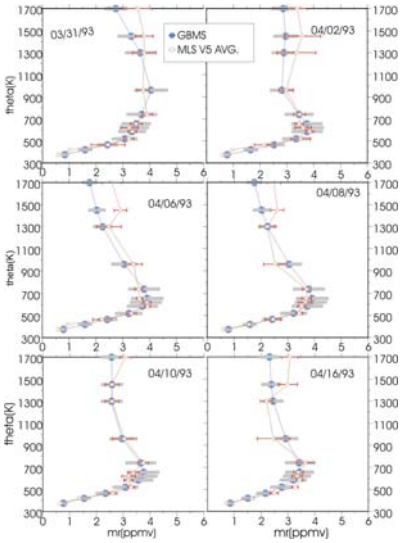

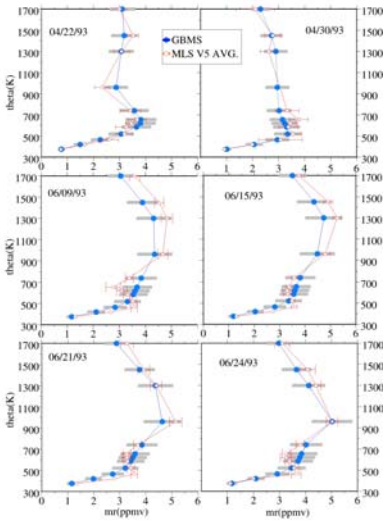

Fig. 1a-b. Vertical mixing ratio profiles for O_3 retrieved from the GBMS, compared with those retrieved by the MLS on UARS for various dates in 1993. MLS profiles are constructed from trajectory-traced air parcels as explained in the text. In the lower stratosphere, adjacent data points are spaced at less than the vertical resolution of either instrument and are therefore not independent of one another in the retrieval processes.

Three features stand out in Figure 1: For MLS and GBMS data at $\theta \leq 900$ K, agreement is generally quite good, and well within the mutual overlap of error bars; for $\theta \geq 1100$ K, agreement is significantly poorer, with MLS profiles generally showing more O_3 than GBMS profiles; the better vertical resolution of the MLS retrievals often picks up a double peaked structure in the 700 K altitude range when it is more rarely seen in the sampling of GBMS data involved here. (Note that this double-peaked structure was more prominent in the full 1993 and 1995 GBMS data sets described by Cheng et al. [4,5]). We will return to these points below.

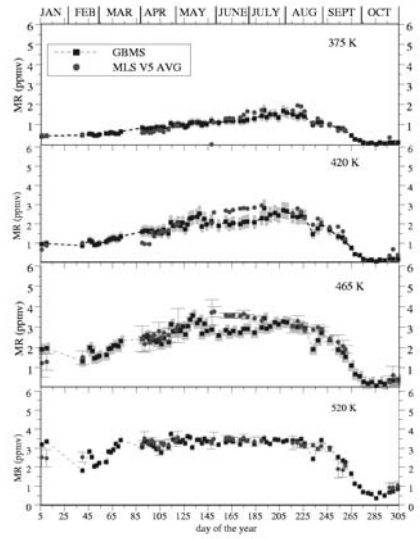

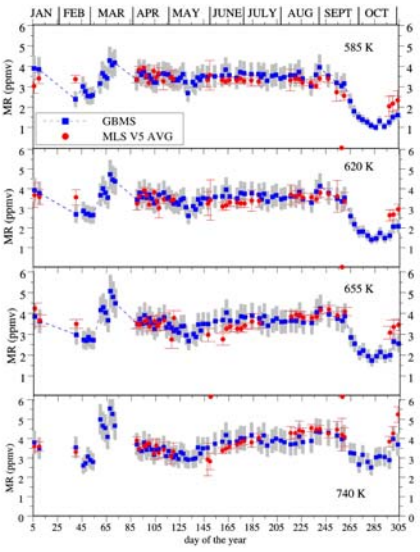

Fig. 2a- b. Time series of O_3 mixing ratios retrieved by GBMS and by MLS during 1993 at various potential temperature levels. MLS mixing ratios are time and distance-weighted averages over all observations lying within 20° longitude x 5° latitude of the daily midpoint of the average trajectory. See the text for details. Dashed lines represent significant time spans when there is no GBMS data. South-looking MLS data are only available in alternate intervals of ~36 day length.

Fig. 2a -b presents ozone time series comparisons for various potential temperature surfaces. To compare the MLS V5 averaged data with GBMS observations, it is plotted on the same day as the GBMS data, although it may have been observed by the MLS up to 6 days earlier or later. At 375 K, agreement is generally quite good throughout the year, although at this level MLS data is beginning to be dominated by climatological a-priori input, while GBMS data is almost entirely determined by a-priori South Pole ozonesonde profile input at this level. Note that the MLS a priori climatology for ozone in the 70-80° S range appears to be rather close to the reality of O_3measured over the Pole.

A steady increase in ozone at altitudes below 520 K is apparent in Figure 2a in both the MLS and GBMS records, beginning about the end of February (starting before polar sunset) and continuing until early August. This is a manifestation of downward transport of air with larger O_3 mixing ratios from higher altitudes, as the winter vortex forms and cooling and subsidence progress. Note, however, that at ~520 K and above, the ozone mixing ratio takes a dip in April and May that is slight at ~740 K but quite pronounced in the 960-1450 K range, after which there is a strong increase to approximately the mixing ratios seen prior to the dip. Little or no attention has been paid to this phenomenon in the literature, though attention was called to it by Cheng et al. [1995, 1996]. We shall return to this in subsection 5.2

At 420 and 465 K, MLS mixing ratios in Figure 2a are notably larger than GBMS values during the midwinter June-July period, but return to close agreement at 520 K, and seldom depart from agreement within the overlap of error bars at higher altitudes, although there is a systematic bias there toward larger MLS values (as in Figure 1). The reason for the mid-winter disagreement in the lower stratosphere is found by close inspection of the profiles in Figure 1. Continued subsidence enhances and compresses the double-peaked structure seen in many ozone profiles and produces a sharp maximum in mixing ratio over a very small vertical range around ~500 K. By June this process has produced peak separations and profile gradients which can still be followed with the greater vertical resolution (~3.5 km) of the MLS instrument and its observing geometry, but are lost at the poorer retrieval resolution of the GBMS, which is limited to ≥7 km for resolving separate layers. By mid-August, although subsidence continues, ozone-hole chemistry is beginning to eat away the lower ozone peak, ultimately eliminating the GBMS two-peak resolution problem.

In the earlier work of Cheng et al. [4] where individual GBMS profiles were given for all observations during 1993, the double-peaked profile structure is seen to be quite prominent in April through May, but the lower peak appears to diminish or disappear in much of the June and July data. With the aid of the MLS data, we can now recognize that this was largely a problem of vertical resolution in the retrieval process, rather than actual loss of the lower peak. This interpretation is confirmed by the comparison of South Pole ozonesonde measurements with MLS and GBMS measurements shown in Figure 3: at 420 and 465 K, MLS and ozonesonde data closely track one another, while the GBMS retrievals at these levels are systematically undervalued only during mid-winter. (Since MLS data are not co-located with these ozonesondes, we have also compared early spring ozonesonde values measured at McMurdo Station (77.9° S, 166.6° E) with MLS average values within a box 20°x5° (longitude x latitude) centered over McMurdo and found excellent agreement - ozonesonde values nearly always within MLS error bars, at all the test levels 465, 520, 585, and 620 K, for 15 comparison days of available data during a test period from Day 234 to Day 260).

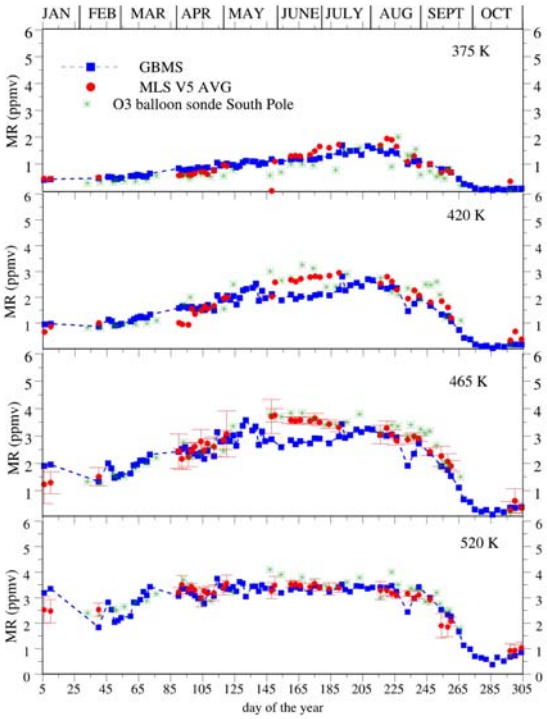

Fig. 3. Time series of mixing ratios as in Figure 2, but for selected levels in the lower stratosphere, compared with South Pole ozonesonde readings. Error bars for GBMS and MLS are as in Figure 2, but omitted here to limit confusion. Note midwinter agreement between ozonesondes and MLS at 420 and 465 K, when GBMS values are systematically and significantly lower. See text for an explanation.

5.2. Origin of the double-peaked profile

We find a double peaked or "notched" structure in almost all of MLS profiles from 70-80° S, as well as in our own South Pole profiles [Cheng et al., 1996] with the exception of the winter period discussed above, when it is lost within the limited GBMS vertical resolution, and during the spring ozone hole period, when the lower peak is destroyed. The double-peaked O_3 profile is thus a large-scale and temporally persistent phenomenon throughout the Antarctic stratospheric vortex.

A "notched" or "double-peaked" structure has been noted on other occasions (where the data were often limited to short periods of observation) in both the

northern and southern polar regions, as referenced by Austin et al. [1], who tried inconclusively to find model mechanisms for this phenomenon. Manney et al. [10] have noted profiles very similar to ours in MLS data, but in their case these were seen to develop during sudden warming events when low-latitude air was advected poleward and trapped in the center of an anticyclonic (cyclonic) region outside, rather than inside, the NH (SH) polar vortex for at least several days. Modeling by Nair et al. [18] and by Morris et al. [14] showed that standard NOx and ClOx catalytic chemistry, coupled with a sharp drop in O_3 photoproduction at high latitudes, appears to account for nearly all the observed O_3 loss in the vicinity of 850-960 K seen by Manney et al. [10]. Neither of these studies extended to altitudes higher than 960 K, (the lower to middle range of the notch) however, but the rapidly decreasing efficiency of the catalytic cycles with increasing altitude presumably determines that a notch, rather than a monatomic decrease, will be the net result for air trapped at high latitudes.

The extra-vortex profiles studied by Manney et al. [10] bear a strong resemblance to those that we find within the vortex, particularly with respect to the altitude of the notch region, although the history of affected air parcels is very different. PV maps (not shown) in the vertical range where the notch appears in the data we consider here indicate that a well-formed and roughly circular vortex existed by early May, 1993, centred near the Pole and encompassing the region of MLS measurements poleward of 70° S that are of concern here.

Cheng et al. [3,4] noted a strong depletion of ozone around the fall equinox, extending through the mid to upper stratosphere, in contour plots of ozone mixing ratios versus altitude and time. This has the same cause (a rapid drop in O_3 photoproduction, accompanied by catalytic attack involving primarily NO_x and ClO_x), and lies in the same altitude range, as the phenomenon studied by Nair et al. [15] and Morris et al. [11]. A quite different phenomenon occurs a little later [4,5], and Figure 2 of the present paper] when nearly the same mixing ratios return in the mid to upper stratosphere that were present well before the equinoctial decline. Since there is no local stratospheric production of O_3 over the winter pole, this ozone has to have been replenished by quasi-lateral transport in the mid to upper stratosphere from regions further north. In general these regions contain larger mixing ratios of ozone than were present over the pole in late summer and early fall (see the 10 mb panel of Figure 3) [4], and although NO_x and ClO_x catalysis will also act on air parcels as they move into polar darkness, enough ozone remains at the end of the process to approximately match the early fall values. The replenished layer participates in general subsidence, but as a result of both subsidence and NOx catalysis, a layer of somewhat diminished ozone lies below it, resulting in a strong double-peaked structure that persists through the winter subsidence, until the lower peak is destroyed by "ozone hole" chemistry in the springtime lower stratosphere. In summary, the strong double-peaked structure we note here is thus a result of NO_x and ClO_x catalytic chemistry in the mid to upper stratosphere around the equinox, followed by an increase in meridional poleward transport in winter that restores larger mixing ratios in the mid to upper stratosphere after some subsidence has occurred. The resulting O_3 profile is akin to that of the tropical water vapor "tape recorder" [13] but in this case recording seasonal polar subsidence of ozone (and replenishment by meridional transport), rather than seasonal tropical upwelling of water vapour.

5.3. Comparison of MLS zonal averages with GBMS

Since the GBMS observations are confined to air immediately over the Pole, while the MLS observations have a southern limit of 80° and sample a full 360° circle at this latitude, it is of value to ask how representative either set of measurements are of ozone everywhere within the 70° or 80° S circle. We therefore turn from the intercomparison of ozone in trajectory-selected air parcels to that of zonal averages of MLS observations versus the centrally located GBMS measurements. Results are shown in Figure 5, where zonal averages of MLS data within different latitude rings are compared with both MLS trajectory-limited averages and the GBMS observations at various representative potential temperatures. Note that we now include some MLS data for times when GBMS data were not available (note particularly the MLS data for days 7-43), in order to point out some temporal features of evolution in vortex formation and ozone chemistry.

Agreement is generally close between the GBMS measurements at the Pole, the trajectory-limited MLS values, and the zonally averaged MLS values, particularly at low altitudes. The midwinter differences at 465 K between all MLS values and those of the GBMS have been explained in Section 5.1. Note that during the winter period both zonally averaged and trajectory-selected MLS values closely agree, indicating a large geographical homogeneity in the lower winter vortex poleward of 70°. Important seasonal differences develop at the upper altitudes shown in Figure 5. Strong gradients are seen in the MLS zone averages at $\theta = 960$ and 1300 K for summer and fall (~days 30-115). Cheng et al., [4] in their Figure 3 show that a circularly symmetric gradient in O_3 develops over the Pole at altitudes in the summer. This is due to weak transport at this time and the dominance of photochemistry which tips the equilibrium mixing ratio of O_3 towards smaller values during the summer's 24 hour daylight. The gradient which is established in summer persists at 960 K and above into the fall (~days 85-115) while O_3 is reduced by NO_x and ClO_x catalysis near the equinox, as discussed in Section 5.2. Somewhat smaller and less stable gradients are seen in the August-September period as the vortex begins to break down.

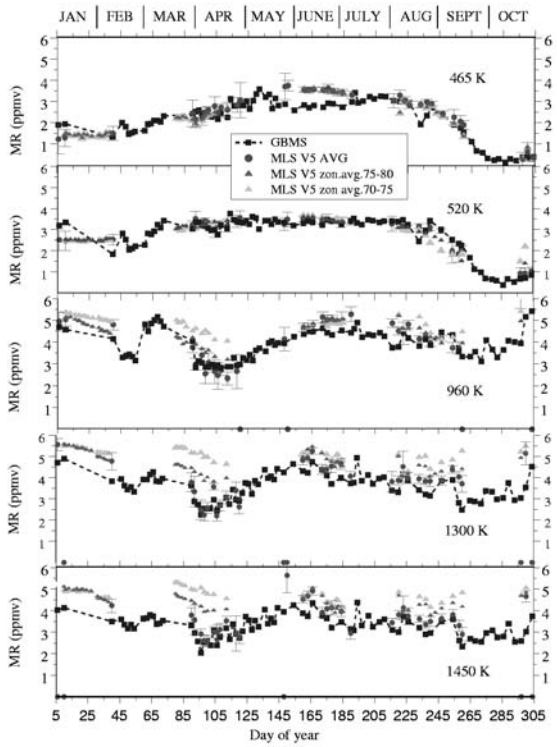

Figure 4. MLS trajectory-traced data (circles) and GBMS data (squares) as in Figure 2, but at selected levels, compared with MLS zonal averages (without trajectory-traced selection of data) for 70°-75° S and 75°-80° S latitude (triangular points). Note that zonal averaging yields MLS average values on days when no trajectory-matched values could be found. At 960 K to 1450 K, persistent strong gradients occur in MLS averages between the 5° zonal bands across the March-April fall equinoctal period, and again with smaller differences and more chaotic behavior across the spring equinoctal period. Note the tight agreement between MLS trajectory-matched and zonally averaged values in the lower stratosphere out to 70° S during the mid-winter vortex period. GBMS values at 465 K are systematically low then due to vertical resolution problems with the sharp O_3 peak that develops at this time. See the text for a discussion.

6. Summary and conclusions

Ground-based O_3 retrievals from the Stony Brook GBMS are generally in good agreement (i.e., well within the mutual overlap of assigned uncertainties) over the altitude range θ ~375-1700 K (~15-41 km) when trajectory tracing is used to select MLS observations for comparison. One exception occurs during the polar winter, when continuing downward transport diminishes the vertical separation between peaks in persistently double-peaked O_3 profiles (and reduces the vertical extent of the O_3 layer associated with each mixing ratio peak). When they are not longer readily resolvable by the deconvolution process associated with the upward-viewing geometry of the GBMS, its retrieved mixing ratios are underestimated. The MLS observing geometry yields about twice the vertical resolution (~3.5 km versus ~7 km) of that obtainable from the GBMS. Ancillary tests show the MLS data maintain a much better match over this altitude range with high-resolution ozonesonde profiles with which we compared them, both at the Pole via trajectory tracing, and on days of concurrent observation in the vicinity of McMurdo Station, Antarctica.

In the mid to upper stratosphere, although there is still general agreement between GBMS and MLS retrievals within the overlap of assigned uncertainties, there is some evidence for systematic biases towards larger MLS values. During summer, fall, and spring, it is likely that at least some of this bias is due to the existence of significant negative poleward gradients in ozone. These gradients are illustrated in a comparison of zone averaged MLS retrievals with GBMS retrievals, where we find significant and persistent negative poleward gradients of ozone existing on constant potential temperature surfaces over 5° latitude intervals in the middle to upper stratosphere (≥ 960 K) in the polar summer and fall, and to a lesser extent in the spring. In winter, these gradients appear to be non-existent or insignificant in the MLS zonal averages at high altitudes between 70°-75° and 75°-80° S, suggesting that at this time a larger degree of homogeneity has been attained in this region of the vortex. Either a small gradient or a systematic retrieval error appears to exist between observations at the MLS 70°-80° S range and those at the Pole, visible at 960 K and higher throughout the winter.

A persistent feature of both GBMS and MLS ozone profiles is the double peaked structure emphasized by Cheng et al. [4]. Starting somewhat before the fall equinox (i.e., polar sunset) O_3 is rapidly depleted over a broad vertical range in the mid to upper stratosphere by NOx and ClOx catalysis in competition with rapidly declining photoproduction. Following this, much larger mixing ratios are again established by increasing poleward transport in the upper stratosphere, which results in a double-peaked profile. During the later fall and winter, the double-peaked structure is compressed in the general subsidence of air within the vortex. During spring and summer, the ozone mixing ratio is increased (relative to winter values) by both transport and photo-production in the mid to upper stratosphere, and the process repeats during the next subsidence. The double-peaked structure, as suggested by Cheng et al. [4], becomes a 'fossil' recording of preceding events, in much the same way that the annual variation of water vapour transport through up-welling into the tropical stratosphere can be traced through alternating layers of increasing and decreasing mixing ratio.

Acknowledgements

This research was supported by NASA through Grant NAG54071 and by the National Research Foundation through Grant OPP9705667. We thank Terry Deshler for access to the University of Wyoming ozonesonde measurements over McMurdo Station in 1993. South Pole ozonesonde measurements were obtained from NOAA, and the 1993 GBMS results were obtained through the

dedication and skill of Curtis Trimble, who wintered over at the Pole to acquire this data. We thank Lucien Froidevaux for useful discussions relating to the MLS data and its use in this analysis, and the entire MLS team for making a wealth of data available to the research community at large.

References

[1] J. Austin, D. J. Hofmann, N. Butchart, S. J. Oltmans, Geophys. Res. Lett., **22**, 2489 (1995).
[2] N. Buchart, E. E. Remsberg, J. Atmos. Sci. **43**, 1319 (1986).
[3] D. Cheng, "Analysis of Ground-based Millimeter-wave Observations of Ozone at the South Pole through two Quasi-Annual Cycles", Ph. D. Thesis, State University of New York, Stony Brook, N.Y., 1996
[4] D. Cheng, R. L. de Zafra, C. Trimble, J. Geophys. Res. **101**, 6781 (1996).
[5] D. Cheng, S. Crewell, U. Klein, R. L. de Zafra, R. A. Chamberlin, J. Geophys. Res. **102**, 6109 (1997).
[6] D. M. Cunold, L. Froidevaux, J. M. Russell, III, B. J. Connor, A. E. Roche, J. Geophys. Res. **101**, 10,335 (1996).
[7] L. Froidevaux, W.G. Read, T. A. Lungu, R. E. Cofield, E. F. Fishbein, D. A. Fowler, R. F. Jarnot, B. P. Ridenoure, Z. Shippony, J. W. Waters, J. J. Margitan, I. S. McDermid, R. A. Stachnik, G. E. Peckham, G. Braathen, T. Deshler, J. Fishman, D. J. Hofmann, S. Oltmans, J. Geophys. Res., **101** 10,017-10,060, (1996).
[8] D. L. Hartman, L. E. Heidt, M. Lowenstein, J. R. Podolske, J. Vedder, W. L. Starr, S. Strahan, J. Geophys. Res. **94**, 16,779-16,795 (1989).
[9] A. M. Lee, H. K. Roscoe, A. E. Jones, P. H. Haynes, E. F. Shuckburgh. M. W. Morrey, H. C. Phmphrey, J. Geophys. Res., **106**, 3203-3211, (2001).
[10] G. L. Manney, L. Froidevaux, J. W. Waters, R. W. Zurek, J. C. Gille, J. B. Kumer, J. L. Mergenthaler, A. E. Roche, A. O'Neill, R. Swinbank, J. Geophys. Res. **100**, 13,939-13,950 (1995).
[11] G. A. Morris, M. R. Schoeberl, L. C. Sparling, P. A. Newman, L. R. Lait, L Elson, J. Waters, R. A. Suttie, A. Roche, J. Kumer, J. M. Russell, III, J. Geophys. Res. **100**, 16,491-16,505 (1995).
[12] G. A. Morris, J. F. Gleason, J. Ziemke, M. R. Schoeberl, J. Geophys. Res., **105**, 17,875-17,894 (2000).
[13] P. W. Mote, K. Rosenlof, M. E. McIntyre, E. S. Carr, J. C. Gille, J. R. Holton, J. S. Kinnersley, H. C. Pumphrey, J. M. Russell III, J. Waters, J. Geophys. Res., **101**, 3989-4006, (1996).
[14] G. Muscari, M. Santee, R. de Zafra, Intercomparison of stratospheric HNO3 measurements over Antarctica: Ground-based millimeter-wave versus UARS/MLS Version 5 retrievals, J. Geophys. Res., (submitted) 2002.
[15] H. Nair, M. Allen, L. Froidevaux, R. W. Zurek, J. Geophys. Res. **103**, 1555-1571 (1998).
[16] A. Nemuc, "Ground-Based Millimeter-Wave Observations of Ozone at the South Pole and a Comparison with UARS/MLS Observations", M.S. Thesis, State University of New York at Stony Brook, May, 2001.
[17] A. Parrish, R. L. de Zafra, P. M. Solomon, J. W. Barrett, Radio Sci., **23**, 106-118 (1988).
[18] J. E. Rosenfield, M. R. Schoeberl, J. Geophys. Res., **106**, 33,485-33,497 (2001).
[19] M. R. Schoeberl, L. R. Lait, P. A. Newman, J. E. Rosenfeld, J. Geophys. Res. **97**, 7859-7882 (1992).
[20] M. R. Schoeberl, L. C. Sparling, Trajectory modeling, in "Diagnostic tools in atmospheric physics", Proceedings of the international school of physics "Enrico Fermi", pp. 289-305, IOS Press, Amsterdam, 1995.
[21] S. E. Strahan, J. E. Nielsen, M. C. Cerniglia, J. Geophys. Res., **101**, 26,615-26,629, 1996.
[22] WMO, "Assessment of trends in the vertical distribution of ozone", WMO Ozone Report No. 43, eds. N. Harris, R. Hudson, and C. Phillips, 1998.

*Corresponding author: anca@inoe.inoe.ro